Electrochimica Acta 56 (2011) 5210–5213

Contents lists available at ScienceDirect

Electrochimica Acta

journal homepage: www.elsevier.com/locate/electacta

High rate performance of virus enabled 3D n-type Si anodes for lithium-ion batteries

Xilin Chen[a], Konstantinos Gerasopoulos[b], Juchen Guo[a], Adam Brown[c], Reza Ghodssi[b], James N. Culver[c], Chunsheng Wang[a,*]

[a] Department of Chemical & Biomolecular Engineering, University of Maryland College Park, MD 20742, USA
[b] Department of Materials Science and Engineering, Institute for Systems Research, Department of Electrical and Computer Engineering, University of Maryland College Park, MD 20742, USA
[c] Institute for Bioscience and Biotechology Research, Department of Plant Science and Landscape Architecture,University of Maryland College Park, MD 20742, USA

ARTICLE INFO

Article history:
Received 2 February 2011
Received in revised form 10 March 2011
Accepted 11 March 2011
Available online 21 March 2011

Keyword:
N-type Si
Lithium-ion battery
Tobacco mosaic virus
Rate performance
3D structure

ABSTRACT

A patterned 3D Si anode is fabricated by physical vapor deposition of n-type Si on a self-assembled TMV1cys-structured nickel current collector. The combination of the large surface area conferred by the virus-enabled 3D Ni/TMV1cys current collector with the high electric conductivity of n-type Si rods results in excellent cyclic stability and rate capability for the core-shell n-type Si/Ni/TMV1cys anodes. Electrochemical impedance spectroscopy reveals that the high electronic conductivity of n-type Si significantly reduces charge transfer resistance, thus even at high current densities the capacity of the n-type Si is increased to almost 630 mAh/g compared to undoped Si.

1. Introduction

In the past decade, the demand for energy-storage technologies for emerging portable electronic devices and fuel-efficient vehicles has placed tremendous interests on the need to improve lithium ion batteries in terms of their energy density, power density, cycle life, safety, and cost. The primary commercial anodic material for lithium ion batteries is graphite with a capacity of 372 mAh/g. Si has been identified as a potential anode material for next-generation lithium ion batteries due to its high capacity of ~3572 mAh/g ($Li_{15}Si_4$) at room temperature, which is almost 10 times the capacity of graphite. However, the high volume changes during the lithiation and delithiation processes induces severe electrode structure failure, resulting in rapid capacity fade. Technologies based on nano-structured materials have been used to increase the stability and rate performance of the Si anode. Magasinki et al. [1] used a CVD technique to fabricate a hierarchical structure by depositing nanosized Si on carbon black particles, forming rigid spherical granules. The particle's internal porosity can accommodate the large volume changes of Si during lithiation and delithiation, enabling high capacity (1950 mAh/g) and stable cycling performance. Using a versatile method, Kim et al. [2] demonstrated high initial specific capacity (2158 mAh/g) of 3D nano-porous Si/carbon anodes and good stability up to 100 cycles. This interconnected 3D porous structure enables fast lithium-ion mobility leading to superior rate performance while the pores in Si particles act as a "buffer layer" that alleviate the volume changes during lithiation and delithiation, leading to good cycling stability. In addition to 3D porous Si/C particles, 1D core-shell nanowires that use carbon [3,4], carbon nanotubes [5], and crystalline Si [6] as cores and Si as a shell, were also investigated to achieve high rate performance and long cycling life. To ensure a good connection between nano-Si and current collector, Si nanowires were well-patterned on a stainless steel substrate by Chan et al. [7] using a CVD method with silane gas as the Si source. Since the free spaces among the Si nanowires can accommodate the volume change of Si nanowires, a high capacity of 3200 mAh/g for nano-Si wires can be stabilized for 10 cycles. Park et al. [8] reported that the Si nanotubes can achieve even higher initial charge capacity of 3247 mAh/g and superior rate performance. To further enhance the connection area between Si nanowires and current collectors, a 3D current collector architecture with patterned Ni nanowires on a stainless steel substrate was used to develop core/shell Si/Ni anodes [9,10]. The 3D Ni current collectors were fabricated using well-patterned genetically modified *Tobacco mosaic virus* (TMV1cys) as a temperate [11]. An exceptional rate capacity and cycling stability were achieved using this novel Si/Ni/*TMV1cys* anode architecture [9,10].

* Corresponding author. Tel.: +1 301 405 0352; fax: +1 301 314 0523.
E-mail address: cswang@umd.edu (C. Wang).

0013-4686/$ – see front matter © 2011 Elsevier Ltd. All rights reserved.
doi:10.1016/j.electacta.2011.03.037

The *Tobacco mosaic virus* (*TMV*) is a plant virus with cylindrical structure, 300 nm in length, 18 nm in outer diameter, and 4 nm in inner diameter. Genetic modification introduces cysteine residues (amino acids with thiol groups) in the virus coat protein structure and enables patterning of the *TMV* onto metal substrates as well as enhanced metal coating in electroless plating solutions due to strong, covalent-like interactions between the thiol groups of the cysteines and metal. [12] The *TMV1cys,* containing one exposed cysteine residue per coat protein subunit yielding ~2100 cysteine residues per virus particle, can self-assemble onto gold substrates vertically due to the surface exposure of the engineered cysteine-derived thiol groups at the 3′ end of the *TMV1cys* rods. [11]. *TMV1cys* has been used as template to fabricate 3D current collectors to enhance the rate performance and cycling stability of Li-ion batteries [9–11,13,14]

In previous Si/Ni/*TMV1cys* anodes, the electron transport between Si and Ni current collector was shown to be greatly enhanced. This likely makes the charge transfer resistance or the electronic conductivity of the Si film the limiting step for rate performance since the charge transfer reaction occurs on the interface between Si and electrolyte, and the electrons have to transport through the Si film. Although carbon coating on the Si surface can enhance the charge transfer reaction [15–23], the low electronic conductivity of Si would still limit the rate performance of the Si/Ni/*TMV1cys* anodes.

In this work, a phosphorus doped Si (n-type Si) film was deposited onto virus enabled 3D current collectors using a physical vapor deposition technique. The resulting n-type Si anode demonstrates exceptional rate performance, cyclic stability, and capacity because the high intrinsic conductivity of the Si layer not only accelerates electron conduction in Si, but also decreases the charge transfer resistance.

2. Experimental

The detailed process for the fabrication of nickel coated TMV1cys current collectors and Si coating using physical vapor deposition (PVD) has been presented in our previous paper [9]. All the synthesis parameters have been kept similar, except for the use of an n-type Si target (Kurt J. Lesker Company, USA) and deposition times (60 min). The n-type Si loading was on the order of 30 $\mu g/cm^2$ after 60 min deposition. The electrochemical performance of patterned Si electrodes is tested in a coin cell using lithium metal as the counter electrode and 1 M $LiPF_6$ in EC/DEC (1:1 by volume) as electrolyte (Novolyte technologies, OH, USA). The charge/discharge behaviors of Si anodes were investigated using Arbin BT2000 (Arbin Instruments, TX, USA) workstation in a voltage windows of 0.02–1.5 V. The lithium insertion/extraction kinetics of Si anodes was characterized by electrochemical impedance spectroscopy using Solartron 1260/1287 electrochemical interface (Solartron Analytical, UK). Structure studies were performed by XRD on D8 Advance with LynxEye and SolX (Bruker AXS, WI, USA) and scanning electron microscopy on a Hitachi (Tokyo, Japan) SU-70 HR-SEM with FFT images.

3. Results and discussion

The n-type Si/Ni/TMV1cys anodes were prepared by physical vapor deposition of n-type Si target on a 3D Ni/TMV1cys current collector. The 3D Ni/TMV1cys current collector was fabricated by chemical deposition of a Ni layer onto patterned TMV1cys which stand nearly vertical on stainless steel (SS) substrates [9,10]. In Ni/TMV1cys nanorods, diameter of TMV1cys core is around 18 nm, and nickel shell is around 40–80 nm, and Ni/TMV1cys nanorods are patterned very well on the substrates to form 3D current collector [9,10]. The length of Ni/TMV1cys varies from 300 nm for a single TMV1cys to 900 nm for three self-aligned particles [9,10]. After 60-min physical vapor deposition, n-type Si/Ni/TMV1cys nanorods with diameters of around 300 nm are well patterned on the substrates to form 3D n-type Si anode as demonstrated by a top-view SEM image of n-type Si/Ni/TMV1cys in Fig. 1. Most n-type Si/Ni/TMV1cys nanorods attach on the stainless steel substrates vertically.

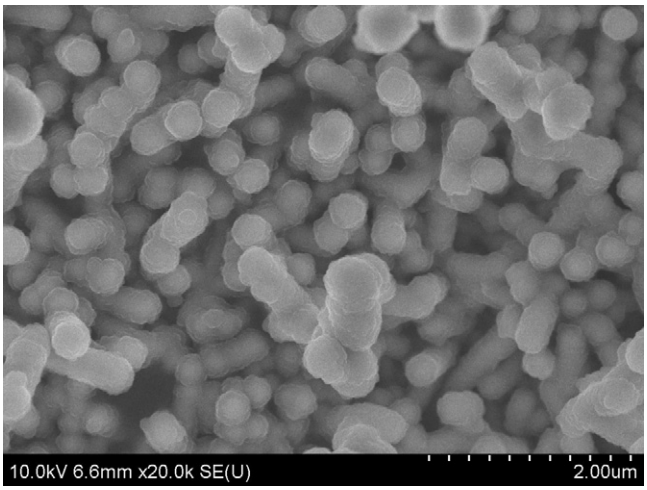

Fig. 1. SEM image of the 3D n-type silicon anode.

The crystal structure of the deposited n-type Si was investigated by XRD. For comparison, an undoped-Si film deposited similarly was also investigated. As shown in Fig. 2, there are not any characteristic peaks for n-type Si or undoped Si, and only background signals for Ni/TMV1cys/SS are present. This indicates that the PVD deposited undoped Si and n-type Si films are amorphous. The characteristic peaks for the 3D Ni/TMV1cys/SS current collector in Fig. 2 are identified and are consistent with PDF # 00-47-1417 for Fe–Ni alloy.

Conductivity of deposited amorphous undoped Si and n-type Si films was measured using a block electrode. The block electrodes were fabricated by deposition of Si or n-type Si films onto a smooth stainless substrate, followed by a silver paste coating on top of Si film as demonstrated in Fig. 3. The thickness of the deposited undoped Si (or n-type Si) film is ~50 nm. The electric conductivity of the deposited n-type Si and undoped-Si were obtained by mea-

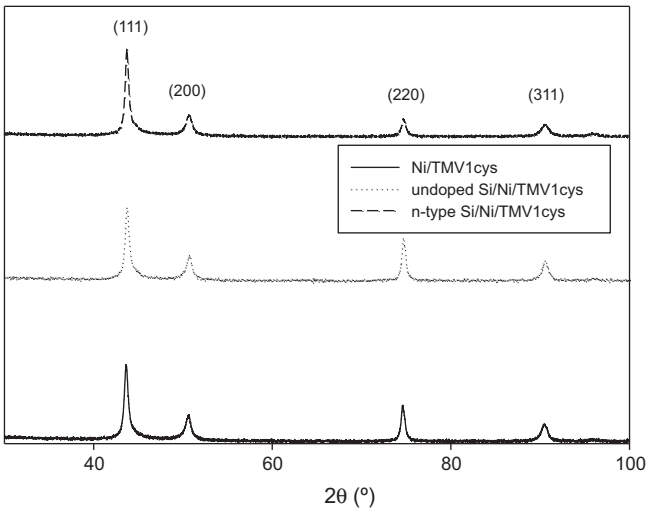

Fig. 2. XRD patterns for Ni/TMV1cys, undoped Si/Ni/TMV1cys, and n-type Si/Ni/TMV1cys.

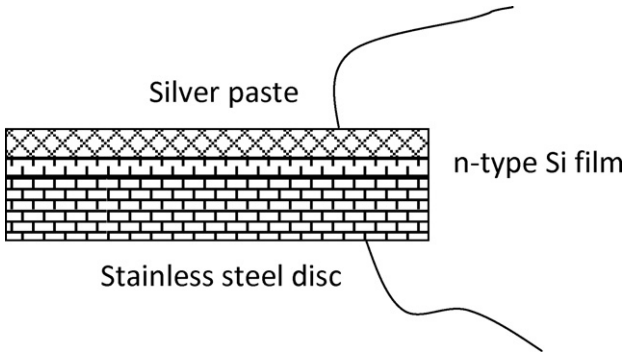

Fig. 3. Schematic diagram of the sandwich SS/Si/Ag layers for Si conductivity measurements.

suring the impedance of Si film using a Solartron 1260/1287. The conductivity was calculated using the equation, $\sigma = \frac{L}{RS}$

The conductivities of n-type amorphous Si and undoped amorphous Si films are determined to be 6.8×10^{-7} S/cm and 4.0×10^{-7} S/cm, respectively, which are much lower than that (>10 S/cm) of the n-type Si target purchased from Kurt J. Lesker Company and the undoped Si ($\sim 2 \times 10^{-4}$ S/cm [24]) targets. The decreases in conductivities may attribute to the structural changes from crystalline to amorphous, as well as changes in the concentration of dopant in n-type Si during physical vapor deposition. However, the conductivity of n-type Si film is still 1.7 times higher than that of undoped Si film. This result is in good agreement with results in open literatures [25–27].

Fig. 4 shows the capacity stability of a n-type Si/Ni/TMV1cys anode during charge/discharge in a voltage between 0.02 and 1.5 V at 2000 mA/g. A non-zero low cut-off voltage is used to avoid lithium deposition during the lithiation process. The initial irreversible capacity is high (42.5%), but it sharply decreases to 3.6% in the second cycle and less than 1% after four cycles. The high irreversible capacity in the first cycle is possibly due to the formation of a solid electrolyte interphase (SEI) film and reduction of oxides induced during the nickel electroless deposition and sample transportation [9]. The initial charge capacity reaches 3535 mAh/g, which is much higher than the initial capacity (2962 mAh/g) of undoped Si/Ni/TMV1cys. The increased capacity of n-type Si anode at 2000 mA/g may be due to the high electronic conductivity of n-type Si compared to undoped Si at the same cycling current rate. Even after 90 charge/discharge cycles, a capacity of 2150 mAh/g,

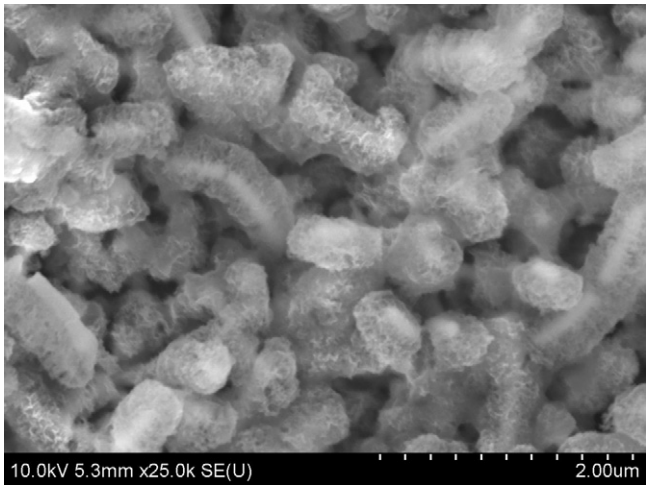

Fig. 4. Cyclic performance of a coin cell using n-type Si/Ni/TMV1cys as the working electrode and lithium metal as the counter electrode.

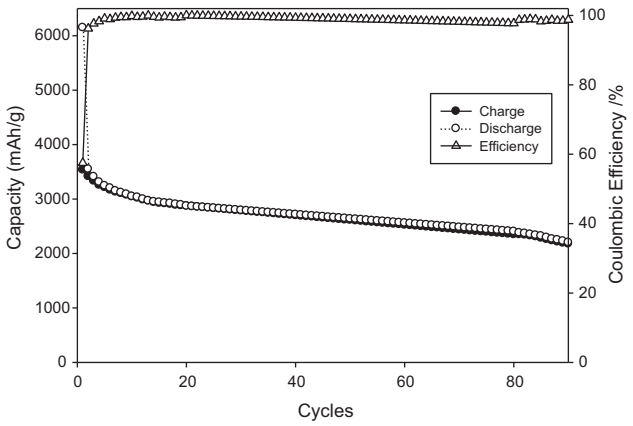

Fig. 5. n-type Si electrode structures after 75 repeating cycles at 2000 mA/g.

is still maintained, which is about 6 times the capacity of a commercial graphite anode. The capacity loss per cycle is about 0.4%. The high cycling stability of the n-type Si/Ni/TMV1cys anodes is due to formation of nano-porous Si structure during lithiation and delithiation cycles, which is similar to undoped Si [9]. Fig. 5 demonstrates that the n-type Si layer swells 3–4 times in volume after 75 cycles, however, the structure maintains its integrity. Voids between the nanorods are believed to accommodate the significant volume change of the n-type Si and thus efficiently alleviate the pulverization of the n-type Si film during the lithiation and delithiation processes. The free space in the electrode structure efficiently relieves the strain and stress during the expansion and shrinkage.

The effect of electrode conductivity on the rate capacity was also investigated by comparing the rate performance of n-type Si and undoped-Si on the Ni/TMV1cys current collector. Fig. 6 shows the rate performance of n-type Si/Ni/TMV1cys and undoped Si/Ni/TMV1cys anodes at different current densities. To ensure the reliability of the reported readings, the batteries were tested for 20 cycles at each current densities. The capacity at every current density is very stable except the initial few cycles. As shown in Fig. 6, the n-type Si/Ni/TMV1cys shows average charge capacities of 3019, 2362, 1593, 650, and 2165 mAh/g at 2000, 4000, 16000, 64000, and 2000 mA/g, respectively; the undoped Si/Ni/TMV1cys shows average charge capacities of 2568, 1749, 642, 37, and 1625 mAh/g at 2000, 4000, 16000, 64000, and 2000 mA/g. Comparing the rate performance of n-type Si/Ni/TMV1cys and undoped Si/Ni/TMV1cys, the capacity of n-type Si/Ni/TMV1cys is 630 mAh/g higher in average than that of the undoped Si/Ni/TMV1cys at all current densities. This indicates that the high electric conductivity of n-type Si

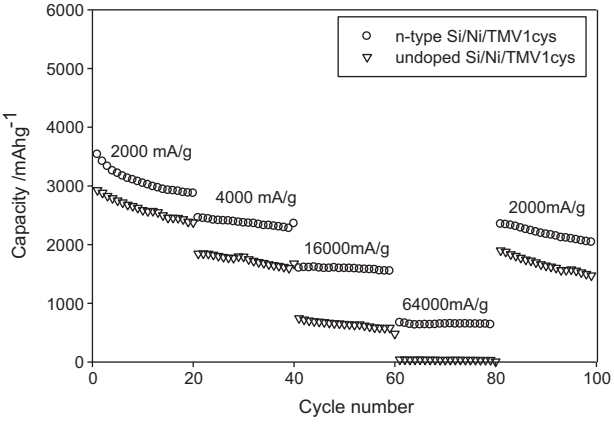

Fig. 6. Rate performances of n-type Si/Ni/TMV1cys and undoped Si/Ni/TMV1cys anodes at various current densities.

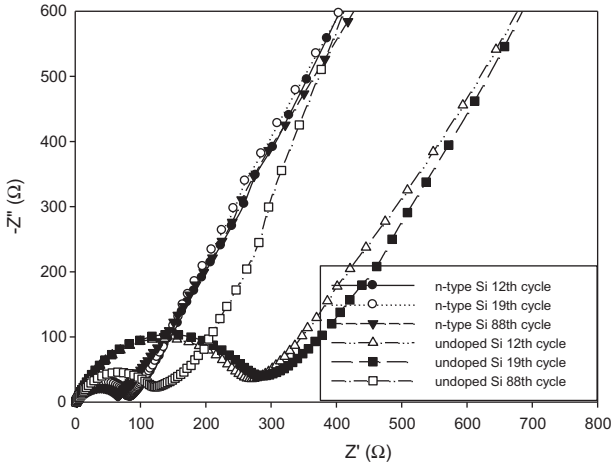

Fig. 7. Electrochemical impedance spectroscopy data for anodes with n-type Si/Ni/TMV1cys and undoped Si/Ni/TMV1cys.

improves the rate performance of n-type Si anodes since both anodes were fabricated using the same parameters. Specifically, the capacity of undoped Si/Ni/TMV1cys is close to zero at 64000 mA/g, but that of the n-type Si/Ni/TMV1cys is 650 mAh/g at the same current density.

The mechanism behind the exceptional rate performance of n-type Si anodes was investigated by comparing the charge/discharge kinetics of the doped and undoped Si anodes using electrochemical impedance spectroscopy. Fig. 7 shows the impedance of n-type Si/Ni/TMV1cys and undoped Si/Ni/TMV1cys at the 12th, 19th, and 88th cycles after fully discharging the cells at 2000 mA/g. All impedance spectra have similar features: a depressed semicircle in high frequency and an inclined line in low frequency. The impedance plot in Fig. 7 is in good agreement with previously reported impedance spectra for Si nanowires [28]. The inclined line in the low frequency region represents the lithium diffusion impedance, while the depressed semicircle consists of interfacial charge transfer impedance at the middle frequency which is overlapped by high-frequency *SEI* film impedance [29]. The detail impedance analysis of n-type Si/Ni/TMV1cys and undoped Si/Ni/TMV1cys electrodes reveals that the *SEI* resistance remains relatively stable after the first cycle, but the charge transfer resistances slightly increase at first, and then decrease after the 19th cycle especially for undoped-Si/Ni/TMV1cys electrodes. The decrease in charge transfer resistance after the 19th cycle is due to the aforementioned sponge-like structure, which enlarges the charge transfer reaction sites, thus enhancing reaction kinetics [9,30]. However, the charge transfer impedance of n-type Si/Ni/TMV1cys is much smaller than those of undoped Si/Ni/TMV1cys. For example, at 19th cycle, the charge transfer impedance for undoped Si/Ni/TMV1cys is about 280 Ω, but for the n-type Si/Ni/TMV1cys it is only about 85 Ω. This result indicates that the high electronic conductivity of n-type Si not only enhances the electron conduction of Si but also greatly enhances charge transfer kinetics, resulting in a high rate performance and cycling stability.

Acknowledgements

The authors acknowledge financial support from the Department of Energy (DESC0001160) under the project science of precision multifunctional nano-structures for electrical energy storage, Army Research Lab (W911NF1020078), National Science Foundation Nanomanufacturing Program (CMMI-0927693) and Maryland Technology Development Corporation (TEDCO 09102380), as well as the technical support of the Maryland NanoCenter. Dr. Culver also acknowledges the support of the Department of Energy, the Office of Basic Energy Sciences DEFG02-02-ER45975.

References

[1] A. Magasinki, P. Dixon, B. Hertzberg, A. Kvit, J. Ayala, G. Yushin, Nat. Mater. 9 (2010) 353.
[2] H. Kim, B. Han, J. Choo, J. Cho, Angew. Chem., Int. Ed. 47 (2008) 1.
[3] H. Kim, J. Cho, Nano Lett. 8 (11) (2008) 3688.
[4] L.F. Cui, Y. Yang, C.M. Hsu, Y. Cui, Nano Lett. 9 (9) (2009) 3370.
[5] W. Wang, P.N. Kumta, ACS Nano 4 (4) (2010) 2233.
[6] L.F. Cui, R. Ruffo, C.K. Chan, H. Peng, Y. Cui, Nano Lett. 9 (1) (2009) 491.
[7] C.K. Chan, H. Peng, G. Liu, K. Mcilwrath, X.F. Zhang, R.A. Huggins, Y. Cui, Nat. Nanotechnol. 3 (2008) 31.
[8] M. Park, M.G. Kim, J. Joo, K. Kim, J. Kim, S. Ahn, Y. Cui, J. Cho, Nano Lett. 9 (11) (2009) 3844.
[9] X. Chen, K. Gerasopoulos, J. Guo, A. Brown, C. Wang, R. Ghodssi, J.N. Culver, ACS Nano 4 (9) (2010) 5366.
[10] X. Chen, K. Gerasopoulos, J. Guo, A. Brown, C. Wang, R. Ghodssi, J.N. Culver, Adv. Funct. Mater. 21 (2011) 380.
[11] E. Royston, A. Ghosh, P. Kofinas, M.T. Harris, J.N. Culver, Langmuir 24 (2008) 906.
[12] S. Lee, E. Royston, J.N. Culver, M.T. Harris, Nanotechnology 16 (2005) S435.
[13] K. Gerasopoulos, M. McCarthy, E. Royston, J.N. Culver, R. Ghodssi, J. Micromech. Microeng. 18 (2008) 104003.
[14] K. Gerasopoulos, X. Chen, J.N. Culver, C. Wang, R. Ghodssi, Chem. Commun. 46 (2010) 7349.
[15] M. Yoshio, H. Wang, K. Fukuda, T. Umeno, N. Dimov, Z. Ogumib, J. Electrochem. Soc. 149 (2002) A1598.
[16] N. Dimov, K. Fukuda, T. Umeno, S. Kugino, M. Yoshio, J. Power Sources 114 (2003) 88.
[17] W.-R. Liu, J.-H. Wang, H.-C. Wu, D.-T. Shieh, M.-H. Yang, N.-L. Wu, J. Electrochem. Soc. 152 (2005) A1719.
[18] M. Holzapfel, H. Buqa, F. Krumeich, P. Novák, F.-M. Petrat, C. Veit, Electrochem. Solid-State Lett. 8 (2005) A516.
[19] S.-H. Ng, J. Wang, D. Wexler, K. Konstantinov, Z.-P. Guo, H.-K. Liu, Angew. Chem., Int. Ed. 45 (2006) 6896.
[20] R.D. Cakan, M.-M. Titirici, M. Antonietti, G. Cui, J. Maier, Y.-S. Hu, Chem. Commun. (2008) 3759.
[21] Y.-S. Hu, R. Demir-Cakan, M.-M. Titirici, J.-O. Muller, R. Schlogl, M. Antonietti, J. Maier, Angew. Chem., Int. Ed. 47 (2008) 1645.
[22] Y. Liu, Z.Y. Wen, X.Y. Wang, A. Hirano, N. Imanishi, Y. Takeda, J. Power Sources 189 (2009) 733.
[23] Q. Si, K. Hanai, N. Imanishi, M. Kubo, A. Hirano, Y. Takeda, O. Yamamoto, J. Power Sources 189 (2009) 761.
[24] J. Bauer, F. Fleischer, O. Breitenstein, L. Schubert, P. Wemer, U. Gösele, M. Zacharias, Appl. Phys. Lett. 90 (2007) 1, 012105.
[25] C. Jeong, M. Jeon, K. Koichi, Trans. Electr. Electron. Mater. 9 (1) (2008) 28.
[26] M. Zaghdoudi, M.M. Abdelkrim, M. Fathallah, T. Mohammed-Brahim, R. Rogel, Mater. Sci. Eng. C 26 (2006) 177.
[27] A.R. Stegner, R.N. Pereira, K. Klein, R. Lechner, R. Dietmueller, M.S. Brandt, M. Stutzmann, Phys. Rev. Lett. 100 (2008) 026803.
[28] R. Fuffo, S.S. Hong, C.K. Chan, R.A. Huggins, Y. Cui, J. Phys. Chem. C 113 (26) (2009) 11390.
[29] C. Wang, A.J. Appleby, F.E. Little, J. Electroanal Chem. 497 (2001) 33.
[30] X. Wang, W. Han, ACS Appl. Mater. Interfaces 2 (2010) 3709.